10.17951/aa.2018.73.1.61-80

ANNALES
UNIVERSITATIS MARIAE CURIE-SKŁODOWSKA
LUBLIN – POLONIA

VOL. LXXIII, 2 SECTIO AA 2018

Significance of the receding contact angle in the determination of surface free energy

Michał Chodkowski* and Konrad Terpiłowski

Department of Interfacial Phenomena, Faculty of Chemistry,
Maria Curie-Sklodowska University,
Plac Marii Curie-Skłodowskiej 3, 20-031 Lublin, Poland
**e-mail: michal.chodkowski@poczta.umcs.lublin.pl*

Surface free energy measurements of solids are a very important issue in various fields of science. Many functional, chemical and physical properties of a given material depend on its surface free energy. The basic method of the surface free energy determination are the contact angle measurements.

The aim of this paper was to study the significance of the receding contact angle measurements in the determination of surface free energy of solids. Based on the materials with various surface properties such as glass, mica, silicon wafers and PMMA, the contact angle measurements were proved to be a very important step in the surface free energy calculations. Referring to some commonly used theories, it was proved that considering only the advancing contact angles during the surface free energy calculations leads to its underestimation and incorrect values of its components. Thus, it was found that the receding contact angle is as an important parameter as the advancing contact angle in the surface free energy determination.

Keywords: receding contact angle, equilibrium contact angle, Tadmor's contact angle, CAH, surface free energy.

1. INTRODUCTION

The surface properties of a solid surface are a very important parameter that characterizes its functional properties. They play a key role in many processes around us: in nature, industry or everyday life. One of them is surface free energy, which provides information on the properties of the surface layer of a solid and describes them in a quantitative way.

The surface free energy cannot be measured directly, but it can be estimated based on the measurements of other quantities on the examined surface. Therefore, surface free energy calculations are based on contact angles measurements. The contact angle (θ) is the angle, measured in the so-called three-phase contact point, between the tangent to the liquid (generally a droplet settled on the solid) and the solid surface. The three-phase contact point means point at the edge of the drop where a liquid-vapor interface meets a solid surface. There are many methods for measuring the contact angle. They are divided into static and dynamic ones. In the static methods, the contact area between the liquid and solid does not change due to a deliberate action during measurements. The dynamic methods are based on changing the solid–liquid interfacial area. It can be done for example by moving the liquid surface or changing the volume of the drops. The most common method for measuring the contact angle is the sessile drop technique [1]. It occurs in both static and dynamic variants. In the static version the drop of test liquid is gently settled on the solid surface using a microsyringe. Then with the help of the camera connected to the computer and the special software, the drop shape is analyzed, and the contact angle is calculated. The contact angle obtained in this way is called the advancing contact angle. Using the dynamic method, the measurement is performed in the following way: the drop of test liquid is gently settled on the solid surface using a microsyringe and the advancing contact angle (θ_a) is measured; then a small amount of liquid is sucked into the syringe and receding contact angle (θ_r) is measured. The difference between the advancing and receding contact angles is called the contact angle hysteresis (H):

$$H = \theta_a - \theta_r \tag{1}$$

The contact angle hysteresis occurs on each real surface because of its heterogeneity and roughness [2].

The relationship between the interfacial tensions and the contact angle in the triple-contact point was proposed in 1805 by Thomas Young [3]:

$$\gamma_{lg} cos\theta_Y + \gamma_{sl} = \gamma_{sg} \tag{2}$$

where: γ_{lg} – the liquid/gas interfacial tension, θ_Y – the equilibrium (Young's) contact angle, γ_{sl} – the solid/liquid interfacial tension, γ_{sg} – the solid/gas interfacial tension. This relationship is called the Young's equation. It describes the mechanical equilibrium at the triple-contact point under the action of three interfacial tensions in an ideal system. However, it contains two unmeasurable quantities (γ_{sg} and γ_{sl}), hence the following modification of the equation is applied in practice:

$$\gamma_l cos\theta_Y + \gamma_{sl} = \gamma_s \tag{3}$$

where: γ_l – the surface tension of the liquid, θ_Y – the equilibrium (Young's) contact angle, γ_{sl} – the solid/liquid interfacial tension, γ_s – the surface free energy of the solid.

There are many approaches for surface free energy determination. Many of them are based on the division of surface free energy into components, which are the result of intermolecular interactions of different nature. The basic direction is to divide these interactions into polar and nonpolar ones. In these studies, only three of them will be discussed due to their common applicability.

Owens and Wendt proposed division of the surface free energy into two components and expressing it as a sum of polar and dispersive interactions [4]:

$$\gamma_s = \gamma_s^d + \gamma_s^p \tag{4}$$

where: γ_s – the surface free energy, γ_s^d – the dispersive component, γ_s^p – the polar component. By combining the above equation with the Young equation and the equation describing the work of adhesion, we

can obtain the expression that allows to calculate surface free energy as the geometric mean of both components:

$$\gamma_l(1+\cos\theta) = 2\left(\gamma_s^d\gamma_l^d\right)^{0.5} + 2\left(\gamma_s^p\gamma_l^p\right)^{0.5} \tag{5}$$

where: γ_l – the surface tension of the test liquid, θ – the contact angle, γ_s^d – the dispersive component, γ_s^p – the polar component. Parameters γ_l^d and γ_l^p characterize the test liquids of polar and non-polar character, thus this method is based on the contact angle measurements of two liquids with the known γ_l^d and γ_l^p components of surface tension. For this purpose, the most common set is water and diiodomethane. Then by solving a system of two linear equations in two variables (γ_s^p, γ_s^d) the values of the surface free energy components can be obtained.

Van Oss et al. extended the above theory by the contribution of hydrogen bonds, introducing an acid-base component [5]:

$$\gamma_s = \gamma_s^{LW} + \gamma_s^{AB} \tag{6}$$

$$\gamma_s^{AB} = 2\left(\gamma_s^+ + \gamma_s^-\right)^{0.5} \tag{7}$$

where: γ_s – the surface free energy, γ_s^{LW} – the Lifshitz-van der Waals component, γ_s^{AB} – the acid-basic component, γ_s^+ – the acid component, γ_s^- – the basis component. Thus, it is called the LWAB approach. Analogously to the previous example, by making appropriate transformations we can get an equation with three unknowns (γ_s^{LW}, γ_s^+, γ_s^-). Then, a set of three liquids with known components is taken in order to perform measurements of contact angles. The water-diiodomethane-formamide or water-diiodomethane-glycerol set is the best choice [6]. After that a system of three equations is constructed. By solving the three-by-three system (system of linear equations in three variables) the values of individual components and thus surface free energy value can be obtained. Finally, the individual energy components are calculated as square roots. However, there are cases when one of them (the acid one) is negative [7]. Some physicochemical reasons for this have been studied by Della Volpe and Siboni [8]. As it was suggested by van Oss, the method requires both values to be positive [9] but some derived theories allow for the

components to have negative values [7]. In practice, it is common to take the negative component value as zero. One needs to be aware that this leads to exaggerated basicity and zero acidity of the surface [8]. This is a serious disadvantage of this approach. As a response to this, various modifications of the discussed theory have taken place, particularly for industrial applications [10]. However, more detailed discussion of the problem is beyond the scope of this paper.

Another method (Contact Angle Hysteresis, CAH) was proposed by Chibowski [11]. Unlike the previous ones, it is based on a quantitative analysis of the contact angle hysteresis. This method is based on the measurements of the advancing and receding contact angles using only one test liquid with the known surface tension:

$$\gamma_s = \frac{\gamma_l(1+\cos\theta_a)^2}{(2+\cos\theta_r+\cos\theta_a)} \tag{8}$$

where: γ_s – the surface free energy, γ_l – the surface tension of the test liquid, θ_a – the advancing contact angle, θ_r – the receding contact angle. A detailed explanation of the basics of this method goes beyond the scope of this paper.

As it was noted earlier, the Young's equation describes only idealized systems corresponding to the physically unrealizable model of ideal (smooth and flat) solid surface. Due to the heterogeneity of different genesis, there is the contact angle hysteresis on each real surface. For this reason, it is not possible to measure the equilibrium contact angle – it is experimentally inaccessible [12]. Several solutions have been proposed to obtain an equilibrium contact angle from the measurements so far. One of them is the Tadmor's approach which is the most widely used [13,14]. He proposed an analytical solution based on the line energy associated with the triple phase contact line [15]:

$$\theta_{eq} = arccos\left(\frac{\Gamma_a\cos\theta_a+\Gamma_r\cos\theta_r}{\Gamma_a+\Gamma_r}\right) \tag{9}$$

where: θ_{eq} – the equilibrium (Tadmor's) contact angle, θ_a – the advancing contact angle, θ_r – the receding contact angle; Γ_a and Γ_a are given by:

$$\Gamma_a = \left(\frac{sin^3\theta_a}{2 - 3\cos\theta_a + cos^3\theta_a} \right)^{1/3} \quad (10)$$

$$\Gamma_r = \left(\frac{sin^3\theta_r}{2 - 3\cos\theta_r + cos^3\theta_r} \right)^{1/3} \quad (11)$$

and they are functions of the surface irregularities (defects on the surface). However, there are many papers where only the advancing contact angle is used in order to determine the surface free energy. This is the case when the Owens-Wendt approach [16] or van Oss et al. approach [17-20] is used and only wettability of superhydrophobic surfaces is examined [21]. There are not many cases where advancing and receding contact angles are tested [22], particularly during the surface free energy determination. In this paper, we examined the significance of the receding contact angle during the surface free energy estimation. Different ways of energy calculations for surfaces with various topography were compared.

2. MATERIALS AND METHODS

2.1 Materials

The following reagents were used as test liquids for the contact angle measurements:

- ultrapure water (Milli-Q™, 18.2 MΩ·cm at 25°C),
- diiodomethane (99% *ReagentPlus*®, Sigma-Aldrich, Germany),
- formamide (98%, Sigma-Aldrich, Germany),

In addition, acetone (99%, POCH S.A., Poland) and methanol (99%, POCH S.A., Poland) were also used to prepare some of the surfaces.

The following surfaces were used during the experiment:

- glass (microscope slides, Comex, Wrocław, Poland);
- mica (Conditional Trade, Warsaw, Poland);
- poly(methyl methacrylate), PMMA (Organika S.A., Sarzyna, Poland);
- silicon wafer (Semiconductor Co., Czech Republic).

The contact angles were measured on the plates cut to 20 × 30 mm. Only the mica was detached from its thicker plates and immediately used for measurements. The glass and the silicon plates were cleaned in acetone and methanol in an ultrasonic cleaner, then rinsed with Milli-Q water and dried at 100°C. The PMMA plates after the protective film removal were flushed in a 20% methanol solution in an ultrasonic cleaner for 15 minutes and then rinsed with Milli-Q water. All substrates were stored in the desiccator before the contact angle measurements.

2.2 Methods

The *Digidrop Contact Angle Meter* (GBX, France) apparatus equipped with the thermostatic attachment was used in order to measure contact angles. The measurements were made by the dynamic sessile drop technique as follows: 6µl droplet was settled on the examined surface and the advancing contact angle was measured, then 2µl of water was sucked from the droplet into the syringe and the receding contact angle was measured. The contact angle values were obtained using the *WinDrop++* software. This program requires indication of the droplet baseline, three-phase contact points and the height of the examined droplet. Then, it analyzes its shape and based on the polynomial algorithm using the NURBS (non-uniform rational basis spline) model the contact angle is calculated. This method is suitable also for an asymmetric droplet because the calculated contact angle is an arithmetic average of the right and left sides contact angle. The obtained value is based only on the droplet shape, without any corrections of a gravitational effect, thus the measurement must be made directly when the droplet is settled on the surface. Moreover, this method requires an excellent image quality in the region of the three-phase contact point.

Ten measurements of the pair (advancing and receding contact angles) on each surface were made. Then the obtained results were averaged, and the equilibrium (Tadmor's) contact angle and the standard deviation were calculated on this basis. The above procedure was repeated for each test liquid.

Surface profiles and their roughness were analyzed using an Atomic Force Microscope (AFM). A standard silicon tip and the contact mode were applied. This technique allows the measurement of roughness in a wide range [23] and provides combination of three-

dimensional surface visualization with quantitative measurement. Based on the AFM measurements, mean surface roughness defined by Ra and RRMS for each surface was calculated. The Ra means the arithmetic average of the absolute values of the profile height deviations from the mean line. This parameter gives an overall description of the surface height variations and indicates the average of the absolute value along the profile. It provides a general description of the height variations on the surface. The RRMS means the root mean square average of the profile height deviations from the mean line. However, the both parameters do not provide any information about the slopes, shapes, and sizes of the asperities or about the frequency and regularity of their occurrence [24].

The surface free energy determination was made on the basis of the averaged contact angle values using the van Oss et al. and CAH approaches. Using the first of these, the values of both the advancing contact angle and the equilibrium contact angle were applied. It was done in order to investigate whether the consideration of the receding contact angle (and thus the equilibrium contact angle instead of advancing contact angle) has a significant effect on the energy values.

3. RESULTS AND DISCUSSION

The figure and the graphs below present the results of the glass surface explorations using the AFM technique.

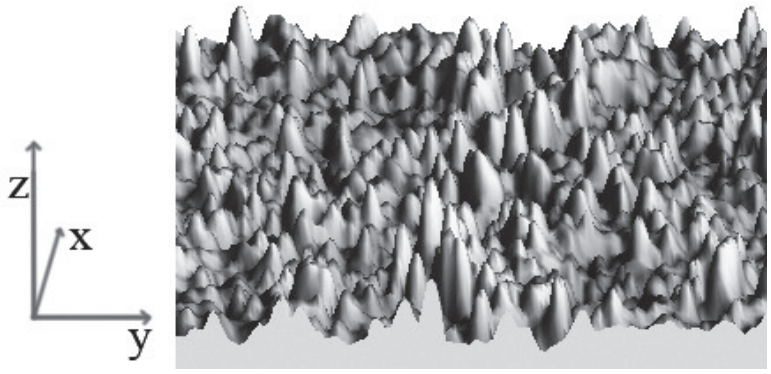

Fig. 1. Three-dimensional AFM mapping of the glass surface (500 nm × 500 nm) with the XYZ axis is shown (the z-axis in nanometers).

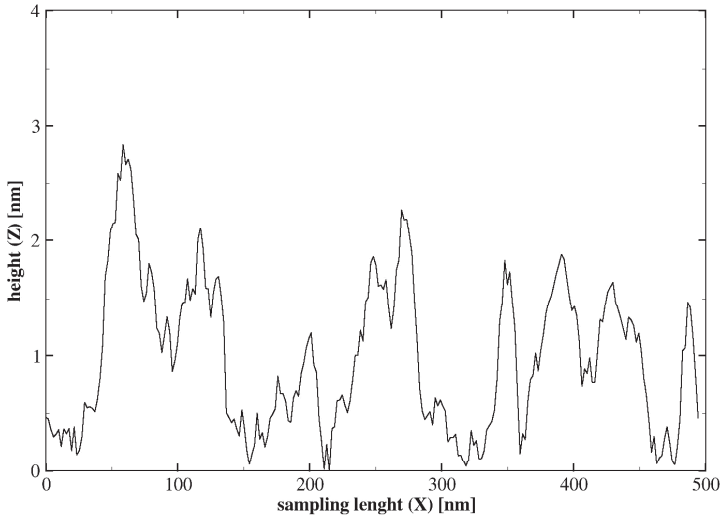

Fig. 2. Profile of the glass surface along the X axis (based on Fig. 1).

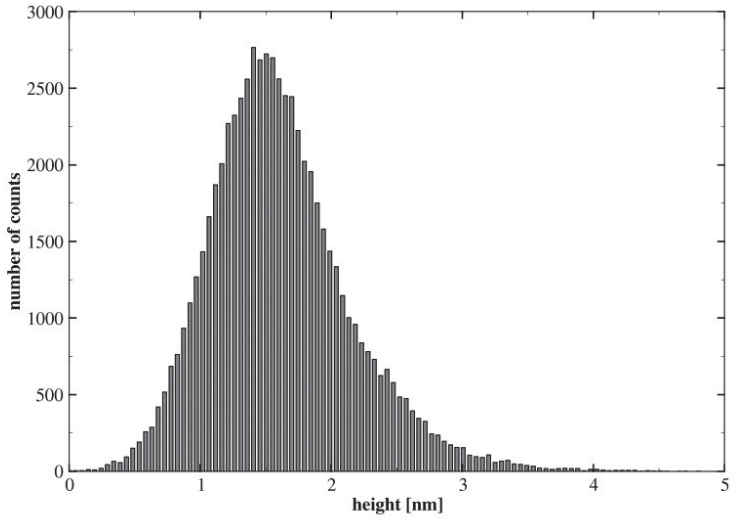

R_a = 1.6 nm; R_{RMS} = 0.54 nm

Fig. 3. Roughness distribution of the glass surface and its roughness parameters.

The glass surface is characterized by the roughness distribution, which is shifted towards higher values. The arithmetic average of the roughness profile (R_a) is equal to 1.6 nm and its root mean square (R_{RMS}) is equal to 0.54 nm. The surface profile shows numerous hollows and wide peaks. However, this is not the most irregular surface among the examined ones.

The values of contact angles of the test liquids on the glass surface and surface free energy are shown in the tables below.

Table 1. Contact angles and hysteresis values on the glass surface.

Contact angle [°]	Liquid		
	water	diiodomethane	formamide
Advancing	31.0±2.0	42.1±1.8	23.5±3.5
Receding	19.8±1.6	32.3±1.6	15.6±2.7
Equilibrium	25.5	37.2	19.7
Hysteresis	11.2±1.8	9.8±1.7	7.9±3.1

Table 2. Surface free energy of the glass.

Approach	Component [mJ/m^2]		
	total	γ_s^+	γ_s^-
van Oss (θ_a)	52.98	1.22	42.81
van Oss (θ_{eq})	54.01	0.91	46.83
	water	diiodomethane	formamide
CAH	66.1	54.9	43.0
CAH (average)		54.7	

As it is shown in Table 2, including the receding contact angle into the surface free energy calculations leads to increase of the energy values (+1,03 mJ/m^2). This can look like a small change, but the values of the components resulting from the van Oss approach also change (significantly in the case of acid component – about 33%). In case of the CAH approach, the average energy value is close to that calculated using the van Oss approach which includes the receding contact angle. Moreover, a large contact angle hysteresis can be observed on the surface. The hysteresis can be explained by large irregularities resulting from the surface roughness.

The figure and the graphs below present the results of the mica surface explorations using the AFM technique.

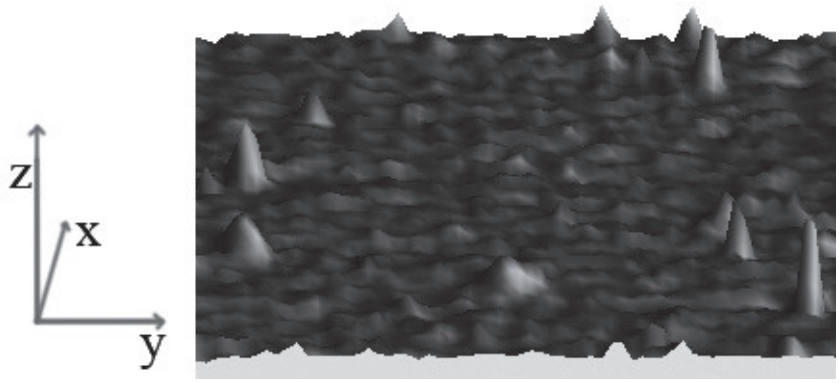

Fig. 4. Three-dimensional AFM mapping of the mica surface (500 nm × 500 nm) with the XYZ axis is shown (the z-axis in Angstroms).

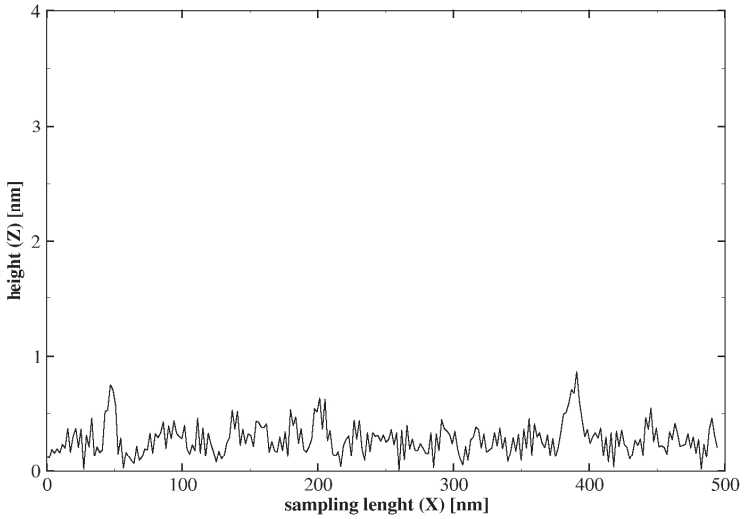

Fig. 5. Profile of the mica surface along the X axis (based on Fig. 4).

The surface mapping of the mica presented in Fig. 4 shows that the mineral does not crack along its crystallographic planes. This fact is visible in the course of the surface profile. It is manifested also by the non-uniform distribution of roughness, which is shifted towards smaller values. This is due to the remains of residual crystallographic surfaces.

The arithmetic average of the roughness profile (R_a) is equal to 0.4 nm and its root mean square (R_{RMS}) is equal 0.14 nm. These parameters indicate that the surface is relatively smooth.

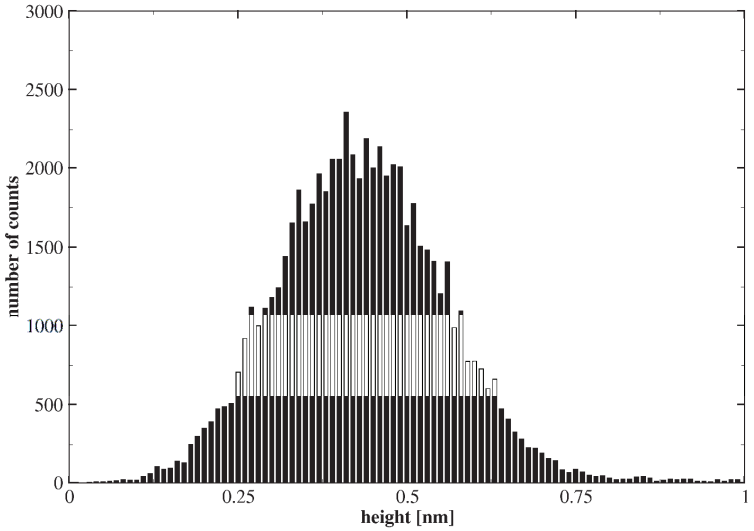

R_a = 0.4 nm; R_{RMS} = 0.14 nm

Fig. 6. Roughness distribution of the mica surface and its roughness parameters.

The values of contact angles of the test liquids on the mica surface and the surface free energy are shown in the tables below.

Table 3. Contact angles and hysteresis values on the mica surface.

Contact angle [°]	Liquid		
	water	diiodomethane	formamide
Advancing	14.9±2.3	28.4±1.4	8.1±1.0
Receding	9.5±1.3	23.1±1.6	3.9±1.3
Equilibrium	12.3	25.8	6.1
Hysteresis	5.4±1.2	5.4±1.5	4.2±1.6

There are low contact angle values on the mica surface. The small hysteresis explains the small differences between the energy values calculated using only the advancing and equilibrium contact angles. However, the energy calculations based on small values of contact angles can be burdened by errors.

Table 4. Surface free energy of the mica.

Approach	Component [mJ/m^2]		
	total	γ_s^+	γ_s^-
van Oss (θ_a)	56.36	0.64	51.56
van Oss (θ_{eq})	56.43	0.53	52.74
	water	diiodomethane	formamide
CAH	71.2	57.6	47.2
CAH (average)		58.7	

The figure and the graphs below present the results of the PMMA surface explorations using the AFM technique.

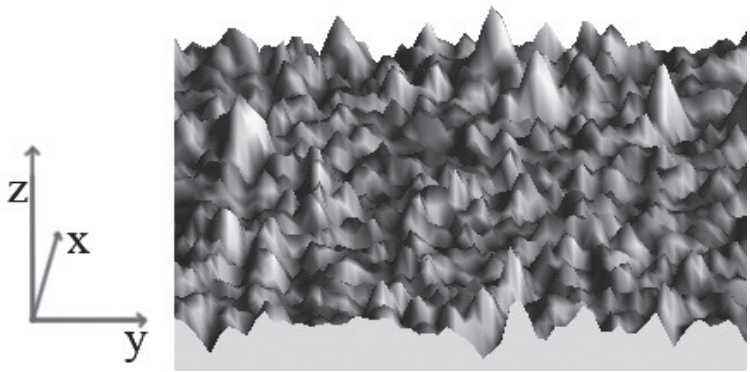

Fig. 7. Three-dimensional AFM mapping of the PMMA surface (500 nm × 500 nm) with the XYZ axis is shown (the z-axis in nanometers).

On the PMMA surface repeating longitudinal grooves are observed. The arithmetic average of the roughness profile (R_a) is equal to 2.7 nm and its root mean square (R_{RMS}) is equal 0.7 nm. These parameters make the surface the roughest of those discussed in the paper.

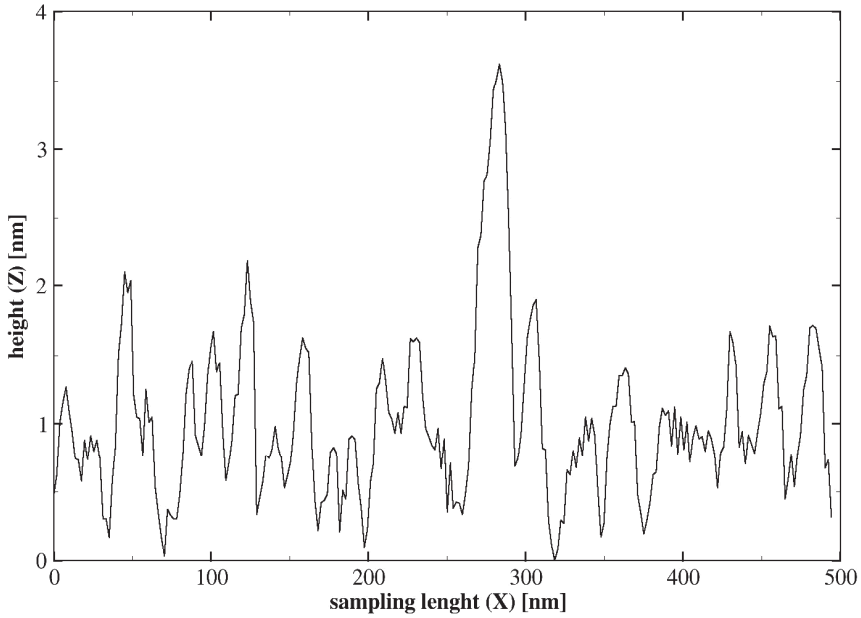

Fig. 8. Profile of the PMMA surface along the X axis (based on Fig. 7).

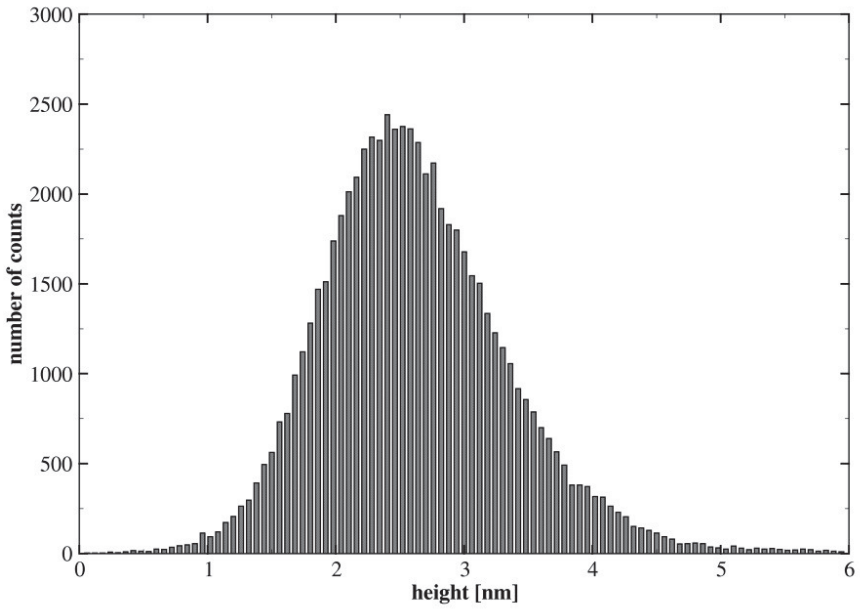

R_a = 2.7 nm; R_{RMS} = 0.7 nm

Fig. 9. Roughness distribution of the PMMA surface and its roughness parameters.

The values of contact angles of the test liquids on the PMMA surface and surface free energy are shown in the tables below.

Table 5. Contact angles and hysteresis values on the PMMA surface.

Contact angle [°]	Liquid		
	water	diiodomethane	formamide
Advancing	73.9±4.0	22.0±1.7	65.3±4.2
Receding	60.5±3.3	15.5±1.3	50.5±3.5
Equilibrium	67.0	18.8	57.8
Hysteresis	10.9±2.9	7.1±1.0	16.1±1.8

Table 6. Surface free energy of the PMMA.

Approach	Component [mJ/m^2]		
	total	γ_s^+	γ_s^-
van Oss (θ_a)	47.17	0.00	17.05
van Oss (θ_{eq})	48.13	0.00	20.38
	water	diiodomethane	formamide
CAH	42.9	38.2	48.5
CAH (average)		43.2	

The results calculated using the van Oss et al. approach are a large generalization because in all cases the square root of acid component (γ_s^+) was negative. Therefore, only the CAH approach (which requires the receding contact angle) can be used in order to determine the surface free energy. The total value obtained using the van Oss et al. approach is in this case only the dispersive component (γ_s^{LW}) of the energy.

The figure and the graphs below present the results of the silicon surface explorations using the AFM technique.

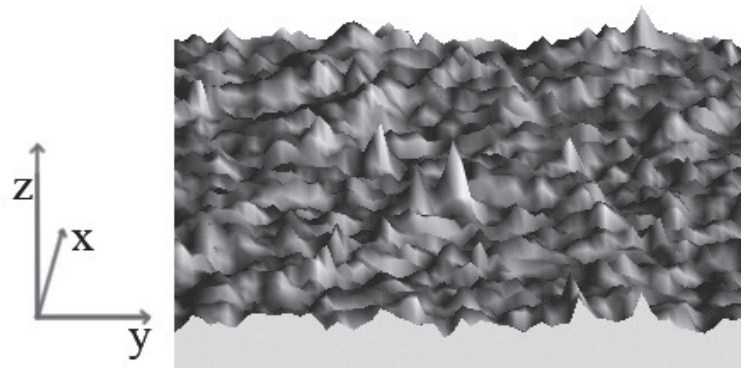

Fig. 10. Three-dimensional AFM mapping of the silicon surface (500 nm × 500 nm) with the XYZ axis is shown (the z-axis in Angstroms).

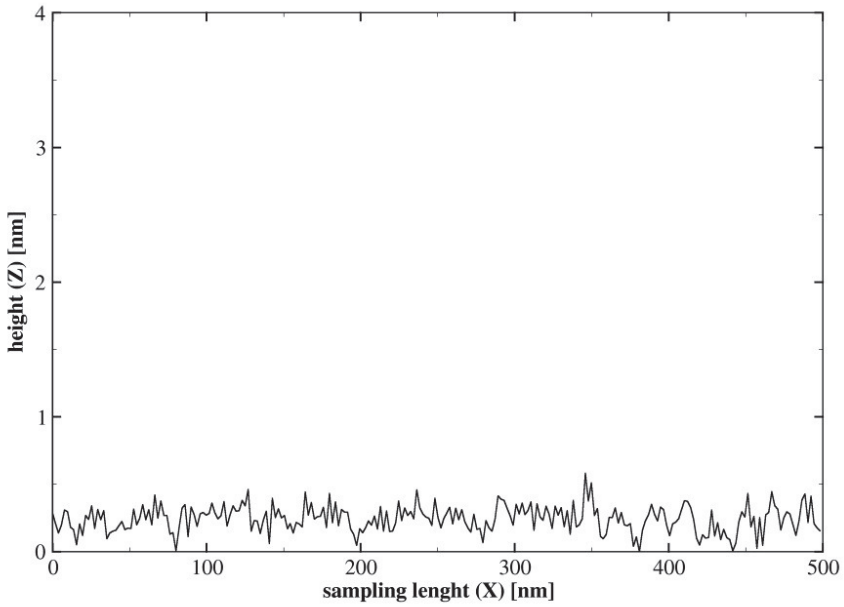

Fig. 11. Profile of the silicon surface along the X axis (based on Fig. 10).

The silicon surface profile along the X axis is uniform, with no clear deviations. The arithmetic average of the roughness profile (R_a) is equal to 0.4 nm and its root mean square (R_{RMS}) is equal to 0.1 nm. Also, the roughness distribution is symmetrical. Thus, the silicon surface is the smoothest of the tested surfaces.

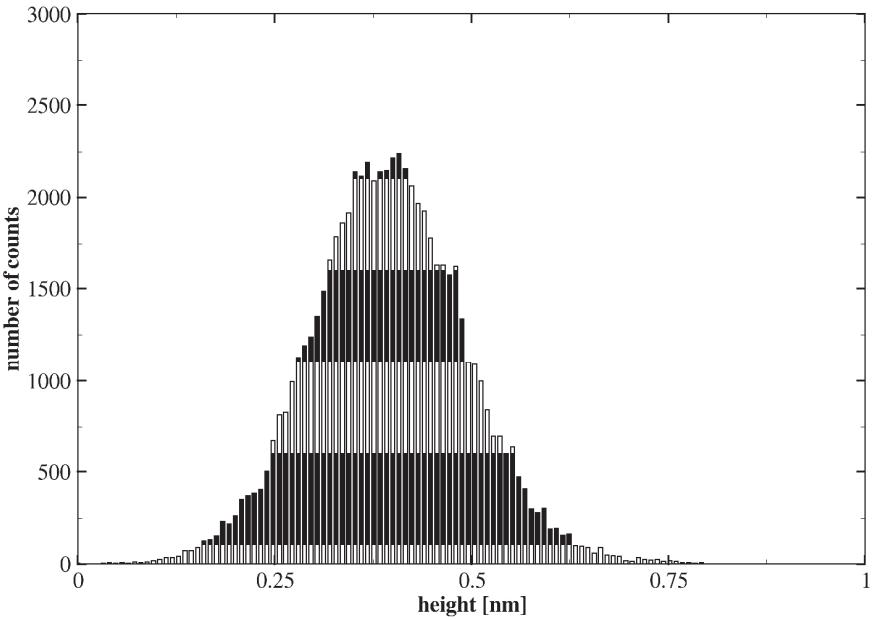

R_a = 0.4 nm; R_{RMS} = 0.1 nm

Fig. 12. Roughness distribution of the silicon surface and its roughness parameters.

The values of contact angles of the test liquids on the glass surface and surface free energy are shown in the tables below.

Table 7. Contact angles and hysteresis values on the silicon wafer surface.

Contact angle [°]	Liquid		
	water	diiodomethane	formamide
Advancing	34.7±1.1	42.2±1.4	34.6±1.0
Receding	24.2±0.9	35.1±2.2	21.5±1.1
Equilibrium	29.5	38.7	28.2
Hysteresis	10.5±1.0	7.1±2.2	13.1±1.1

Table 8. Surface free energy of the silicon wafer.

Approach	Component [mJ/m^2]		
	total	γ_s^+	γ_s^-
van Oss (θ_a)	46.87	0.38	45.97
van Oss (θ_{eq})	50.16	0.52	47.57
	water	diiodomethane	formamide
CAH	64.7	51.4	43.3
CAH (average)		53.1	

As can be seen above when using the van Oss approach the difference in the energy values calculated using only the advancing and equilibrium contact angle is significant. It is also possible to observe differences in the values of the energy components, especially for the acid component.

In the all cases, the measured values of the contact angles of the test liquids and the contact angle hysteresis show that there is no simple relationship between the surface roughness and the contact angle on the surface.

4. CONCLUSIONS

The contact angle measurements are a very important step in the surface free energy calculations. As it was mentioned above, many scientists use static methods, obtaining as a result and taking into consideration only the advancing contact angle. However, it is not an equilibrium contact angle that occurs on a given surface. This is due to the presence of contact angle hysteresis on each real surface.

As it was proved above, considering only the advancing contact angles during the surface free energy calculations leads to its underestimation and incorrect values of its components. The obtained results also depend on the structure and roughness of the tested surfaces. Therefore, it is necessary to measure both advancing and receding contact angles and, on this basis, calculating the

equilibrium contact angle. Then the equilibrium contact angle should be used in the surface free energy calculations. Considering the receding contact angle in the surface free energy calculations using the van Oss et al. approach allows to obtain the equilibrium values.

There are cases when the value of one of the square roots of the component of the van Oss et al. approach is negative. Then only the CAH approach can be used in order to determine the surface free energy. This requires also the receding contact angles measurements.

Noteworthy is the fact that the values of the surface free energy obtained from both approaches encompassing the receding contact angle (van Oss et al. and CAH approaches) do not differ much.

This paper shows that the receding contact angle is as an important parameter as the advancing contact angle in the surface free energy determination.

REFERENCES

[1] Y. Yuan, T.R. Lee, in: Surface Science Techniques (G. Bracco and B. Holst, Eds.), Vol. 51, Springer Berlin Heidelberg, Berlin, Heidelberg, p. 3, 2013.
[2] E. Chibowski, M. Jurak, Colloid and Polymer Science, **291**, 391, (2013).
[3] T. Young, Philosophical Transactions of the Royal Society, **95**, 65, (1805).
[4] D.K. Owens, R.C. Wendt, Journal of Applied Polymer Science, **13**, 1741, (1969).
[5] C.J. van Oss, R.J. Good, M.K. Chaudhury, Langmuir, **4**, 884, (1988).
[6] B. Jańczuk, E. Chibowski, J.M. Bruque, M.L. Kerkeb, F. González – Caballero, Journal of Colloid and Interface Science, **159**, 421, (1993).
[7] K.L. Mittal, F.M. Etzler, Lessons from Surface Science, in: Contact Angle, Wettability and Adhesion (K.L. Mittal, Ed.), Vol. 6, CRC Press, Leiden, Boston, p. 121, 2009.
[8] C. Della Volpe, S. Siboni, Journal of Adhesion Science and Technology, **14**, 235, (2000).
[9] C.J. van Oss, Interfacial Forces in Aqueous Media, Marcel Dekker, New York, 1994.
[10] M. Järn, C.M. Tåg, J. Järnström, B. Granqvist, J.B. Rosenholm, Journal of Colloid and Interface Science, **301**, 668, (2006).
[11] E. Chibowski, Advances in Colloid and Interface Science, **103**, 149, (2003).
[12] E. Bormashenko, Colloid and Polymer Science, **291**, 339, (2013).

[13] L. Makkonen, The Journal of Chemical Physics, **147**, 064703, (2017).
[14] K. Terpiłowski, M. Szaniawska, Adsorption, **25**, 1, (2019).
[15] R. Tadmor, Langmuir, **20**, 7659, (2004).
[16] K. Song, J. Lee, S.O. Choi, J. Kim, Polymers, **11**, 498, (2019).
[17] Y. Danchenko, V. Andronov, M. Teslenko, V. Permiakov, E. Rybka, R. Meleshchenko, A. Kosse, Eastern-European Journal of Enterprise Technologies, **91**, 9, (2018).
[18] E. Kraus, L. Orf, I. Starostina, A. Efimova, R. Perelygina, O. Stoyanov, Polymer Engineering and Science, **58**, 2288, (2018).
[19] C.E. Cornejo, M.E. Bertram, T.C. Diaz, S.R. Narayan, Electronic and Photonic Materials, **57-58**, 3403, (2018).
[20] E. Błońska, A. Klamerus-Iwan, S. Łagan, J. Lasota, Ecohydrology, **11**, 2023, (2018).
[21] Z. Wang, W. Yang, F. Sun, P. Zhang, Y. He, X. Wang, D. Luo, W. Ma, G.C. Sergio, Surface Engineering, **35**, 418, (2018).
[22] G.R. Duursma, K. Sefiane, S. David, Chemical Engineering Research and Design, **88**, 737, (2010).
[23] R.R.L. De Oliveira, D.A.C. Albuquerque, T.G.S. Cruz, F. Yamaji, F. Leite, in: Atomic Force Microscopy - Imaging, Measuring and Manipulating Surfaces at the Atomic Scale (Victor Bellitto, Ed.), p. 147, 2012.
[24] B. Bhushan, Surface Roughness Analysis and Measurement Techniques, in: Modern Tribology Handbook (B. Bhushan, Ed.), Vol. 1, CRC Press, USA, p. 49, 2002.